6

Computational Design of A New Class of Si-Based Optoelectronic Material

Meichun Huang
Dept . of Physics ,Xiamen University ,Xiamen
CCAST (World Laboratory), PO Box 8730, Beijing,
China

1. Introduction

Computational materials science, as an intersection of theoretical physics, condensed matter physics and material science, its main tasks, in general, are firstly, research and calculate the physical and chemical properties for known materials. This would help us to better understand the microscopic mechanism of some material properties and open up new fields of applications. Secondly, computational design of new materials, that would help us to explore and design new materials to meet some proposed requirements. As we known, new material design and development is the basis of high-tech material and its device applications.

The research history of computational materials science can actually be traced back to the mid 20s of last century. Immediately after the birth of quantum mechanics theory, many excellent theoretical works were applied to the study of physical properties of solid materials. In the early years of the computational materials science, it is mainly to adopt semi-empirical method. This is because the object being studied is a many-particle system which contains very large amounts of atoms and electrons. One cannot find the rigorous analytical solutions, but the empirical values of the measurable parameters are available, Therefore, in semi-empirical method, the number of experience parameters is at least as much as that of material types, hence, most studies are pointed only to the computing research category of physical properties. Until the mid 60s of last century, Hohenberg-Kohn (Hohenberg & Kohn. 1964) and Kohn-Sham (Kohn & Sham 1965) proposed the Density Functional Theory (DFT) and Local Density Approximation (LDA), to get rid of the semi-empirical method restriction, and hence causing the birth of so-called *ab initio* or the first principles method that do not depend on experimental parameters. This method has now become a core technology of the computational material science, computational chemistry and computational condensed matter physics and is widely used.

What is a First Principles for the physical world, no one seems to be specified clarify its meaning. Many physicists believe that the most precise description of atoms and smaller than the atomic system is the theory of quantum electrodynamics (QED). Therefore, QED is a theory called first principles of the micro world. In the field of condensed matter physics and materials science, within the framework of the density functional theory, if one do not consider the high-energy radiation correction, one needs only the electromagnetic theory, Schrödinger equation and/or Dirac equation and a few of parameters unrelated to specific

materials, namely, electron mass m and charge e; atomic mass M and charge Z; Bohr radius a_0; Planck constant h and fine structure constant a, so as to describe the various properties of many-particle system. This is referred to the First Principles in this article. In other words, the first principles in the condensed matter physics, in contrast with the basic theory of theoretical physics, it does not involve the physical basis of a more profound question, such as where the electronic mass comes from, why the fine structure constant is approximately equal to 1/137 and whether it changes over time, etc., and consequently, the Principles only consider the 7 parameters to be fixed natural constants.

This chapter is not to simply introduce an *ab initio* calculation for a particular Si-based optoelectronic materials, but also the computational design of the Si-based new materials is presented here. It mainly consists of two steps: at first, we should point out the functional requirements on these new materials such as optoelectronic materials, and put forward the design of the new materials and its basic properties for the requirements: analyze the factors needed to achieve these material requirements, a new material composition, atomic choice and lattice type are designed. Then, we should calculate its electronic structure by using the first principles method and examine whether the results meet the pre-made requirements. Obviously, the semi-empirical methods are often useless because there are no available experimental parameters. If the result is not satisfactory, the designed model, calculation methods and accuracy should be adjusted and improved in next steps.

In this chapter, the design idea, atomic model of materials, and their electronic structure for a new class of silicon-based optoelectronic materials are presented. A summary of the research background, recent progress and problems concerning the Si-based materials is briefly given in Sec.2. Based on this analysis, we propose design of a new silicon-based material with direct band gap is one of the better solutions. However, how to design direct band-gap semiconductor new materials, there is no ready-made principle to be followed. Therefore, a design idea that easier to operate is proposed based on the widely analysis and synthesis of band-gap types for existing semiconductor materials. In fact, the design idea contains only simple physics principle. Though it can be excavated out from piles of existing experimental and theoretical calculated data, up to now, no one has been able to extract it out and give a clear elaboration. The design idea is presented in Sec.3. Our design of new Si-based light emitting materials model and preliminary results are described in Sec.4. The result shows that the design has more clear physical basis and is more compatible with silicon technology. We note that, *ab initio* calculation is good for material properties, but material design needs more advanced physical model to solve the involved physical problem, thus many unnecessary calculation workload may be avoided. In Sec.5, a simple summary is presented.

Our computational design and preliminary results still need experimental validation. There is no doubt that the designed material is an ideal structure coming out from the theoretical calculations, its crystal growing is not an easy task. It will definitely encounter many practical problems to be overcome. Experimental topics will not be discussed in this chapter.

2. Research progress and problems

In this section, the main progress and the existing problems in the field of silicon-based optoelectronic material will be briefly reviewed. It is well known, the development of silicon microelectronics technology in the 20th century is one of the most compelling high-tech

world wide achievements. It has aroused changes almost to all kinds of technology and even most people's daily life. Now, when the Si microelectronics technology becomes more and more close to its quantum limit, there are great challenges on the transmission rate of information and communication technology, also developing ultra-high speed, large capacity optoelectronic integration chip. Thus, the development and research of Si-based optoelectronic materials has become the must topic of major concern in the scientific world.

Since crystal silicon is an indirect band gap semiconductor, the conduction band bottom is located at near X point in the Brillouin zone that has an O_h point group symmetry. The indirect optical transition must have other quasi-particle participation, such as the phonons, so as to satisfy the quasi momentum conservation. We know that ordinary crystal silicon could not be an efficient light emitter, since the indirect transition matrix element is much less than that of the direct transition. For more than 20 years, people have been seeking methods to overcome the shortcomings of silicon yet unsuccessful. However, in recent years, researches show it is possible to change the intrinsic shortcomings of Si-based material. The main strategies include: (a) use of Brillouin zone folding principle (Hybertsen & Schlüter 1987), selecting appropriate number of layers m and n, the super lattices $(Si)_m/(Ge)_n$ can become a quasi-direct band gap materials; (b) synthesis of silicon-based alloys. such as $FeSi_2$, etc. (Rosen ,et al. 1993), the electronic structure also has a quasi-direct band gap; (c) in silicon, with doped rare earth ions to act the role of luminescent centers (Ennen. et al 1983); (d) use of a strong ability of porous silicon (Canham 1990; Cullis & Canham. 1991; Hirschman et al.1996); (e) use of the optical properties of low-dimensional silicon quantum structures, such as silicon quantum wells, quantum wires and dots, may avoid indirect bandgap problem in Si (Buda. et al, 1992); (f) use of silicon nano-crystals (Pavesi, et al. 2000; Walson ,et al 1993) ; (g) silicon/insulator superlattice (Lu et al. 1995) and (h) use of silicon nano-pillars (Nassiopoulos,et al 1996). All these methods are possible ways to achieve improved properties of silicon-based optoelectronic materials.

Recently, an encouraging progress on the experimental studies of the silicon-based optoelectronic materials and devices has been achieved. The optical gain phenomenon in nanocrystalline silicon is discovered by Pavesi's group. (Pavesi, et al. 2000). They give a three-level diagram of nano-silicon crystal to describe the population inversion. The three levels are the valence band top, the conduction band bottom and an interface state level in the band gap, respectively. Absorbed pump light (wavelength 390 nm) enables electronic transitions from the valence band top to the conduction band bottom, and then fast (in nanosecond scale) relaxation to interface states under the conduction band bottom. The electrons in interface states have a long lifetime, therefore can realize the population inversion. As a result the transition from the interface states to the valence band top may lead stimulated emission. In short, the optical gain of silicon nanocrystals in the short-wave laser pump light has been confirmed by Pavesi's experiment.

However, that is neither the procession of minority carriers injected electroluminescence, nor the coherent light output. In fact, nano-crystalline silicon covered with SiO_2 still retains certain features of the electronic structure of bulk Si material with indirect band gap. It is not like a direct band gap material, such as GaAs, that achieves injection laser output. In addition, light-emitting from the interface states of silicon nanocrystals is a slow (order of 10 microseconds) luminous process, much slower than that of GaAs (magnitude of nanoseconds). It indicates that the competition between heat and photon emission occurs during the luminous process. Therefore, the switching time for such kind of silicon light-emitting diode (LED) is only about the orders of magnitude in MHz, whereas the high-

speed optical interconnection requires the switching time in more than GHz. It is still at least 3 to 4 magnitudes slower.

Another development of the Si-based LED is the use of a c-Si/O superlattice structure by Zhang Qi etc (Zhang Q ,*et al*. 2000). They found that it has a super-stable EL visible light (peak of ~2 eV) output. The published data indicates that the device luminous intensity had remained stable, almost no decline for 7 months.This feature is obviously much better than that of porous silicon, and reveals an important practical significance for the developing of silicon-based optoelectronic-microelectronic integrated chips. They believe that if an oxygen monolayer is inserted between the nanoscale silicon layers, it may cause electrons in Si to undergo the quantum constraint. But a theoretical estimation indicates that the quantum confinement effect is very small, and even can be ignored in this case, because the thickness of the oxygen monolayer is too small (less than 0.5 nm). Therefore, the green electroluminescent mechanism in this LED still needs further study.

In addition, an important work from Homewood's group, they investigated a project called dislocation engineering which achieved effective silicon light-emitting LED at room temperature (Ng ,et al. 2001). They used a standard silicon processing technology with boron ion implantation into silicon. The boron ions in Si-LED not only can act the role of *pn* junction dopant, and also can introduce dislocation loops. In this way the formation of the dislocation array is in parallel with the *pn* junction plane. The temperature depending peak emission wavelength of the device (between 1.130-1.15μm) , has an emitting response time of ~18μs, and the device external quantum efficiency at room temperature ~2×10^{-4}. As it's at the initial stage of development, it is a very prospective project worth to be investigated.

After a careful analysis of the luminous process of the above silicon-based materials and devices, it is not hard to find that many of them are concerned with the surface or interface state, from there the process is too slow to emit light. It causes the light response speed to become too slow to satisfy the requirements of ultra-high speed information processing and transmission technology. To fully realize monolithic optoelectronic integrated (OEIC), it needs more further explorations, and more fundamental improvement of the performance of silicon-based optoelectronic materials.

To solve these problems, from the physical principles point of view, there are two major kinds of measures: namely, To try to make silicon indirect bandgap be changed to direct bandgap, and to make full use of quantum confinement effect to avoid the problem of indirect bandgap of silicon. Recently, a large number of studies on quantum wires and dots, quantum cascade lasers and optical properties are presented.

This article is based on the exploration of the band modification. The main goal is to design the direct band gap silicon- based materials, hoping to avoid the surface states and interface states participation in luminous process and to have compatibility with silicon microelectronic process technology.

One of the research targets is looking for the factors that bring out direct bandgap and using them to construct new semiconductor optoelectronic materials. Unfortunately, Although the "band gap" concept comes from the band theory, the modern band theory does not clearly give the answers to the question whether the type of bandgap for an unknown solid material is direct or indirect. To clarify the type of bandgap of the material we should precede a band computation. In fact, the research around semiconductor bandgap problems has been long experienced in half of a century. A summary from the chemical bond views for analysis and prediction the semiconductor band gap has been given in early 1960s by Mooser and Pearson (Mooser & Pearson .1960). In the 1970s, the relations between the

semiconductor bond ionicity and its bandgap are systematically analyzed by Phillips in his monographs (Phillips. 1973). Over the past 20 years, in order to overcome the semiconductor bandgap underestimate problems in the local density approximation (LDA), various efforts have been taken. The most representative methods are the development of quasi-particle GW approximation method (Hybertsen & Louie. 1986 ; Aryasetiawan & Gunnarsson. 1998; Aulbur et al.2000) and sX-LDA method (Seidl , *et al*. 1996), their bandgap results are broadly consistent with the experimental results. Recently, about the time-dependent density functional theory (TDDFT) (Runge & Gross 1984; Petersilka et al. 1996) and its applications have been rapidly developed and become a powerful tool for researching the excited state properties of the condensed system. All of the above important progress have provided us with semiconductor bandgap sources, the main physical mechanism and estimation of bandgap size. They have a clearer physical picture and are considered to be main theoretical basis in the current bandgap engineering.

However, these efforts are mainly focused in the prediction and correction of the band gap size, they almost do not involve the question whether the bandgap is direct or indirect. From the perspective of material computational design, a very heavy and complicated calculation in a "the stir-fries type" job and choosing the results to meet the requirements are unsatisfactory. In order to minimize the tentative calculation efforts, physical ideas must be taken as a principle guidance before the band structure calculations are proceeded. In next Section, a design concept and the design for new material model will briefly be presented

3. Computational design: principles

The complexity in the many-body computation of the actual semiconductor materials rises not only from without analytical solution of the electronic structure, but also lack of a strictly theory to determine their bandgap types. Nevertheless, we believe that the important factors determining a direct band gap must be hidden in a large number of experimental data and theoretical band structure calculations. We comprehensively analyze the band structure parameters for about 60 most commonly used semiconductor, including element semiconductor, compound semiconductor and a number of new semiconductor materials. It was found that there are three major factors deciding bandgap types, namely, the core state effect, atomic electronegativity difference effect and crystal symmetry effect (Huang M.C 2001a; Huang & Zhu Z.Z. 2001b,c, Huang et al. 2002; Huang 2005). Actually, these three effects belong to the important component in effective potential that act on valence electrons. The first two effects have also been pointed out in literature on some previous band calculation, but the calculations did not concern on material design as it's goal. A more detailed description will be given in the following

3.1 Core states effect

First of all, let us consider the element semiconductors Si, Ge and α-Sn. Their three energy at the conduction band bottom relative to the valence band top (set it as a zero energy) with the increase in core state shell in atom, the variation rules are as follows:

1. When going from Si to Sn, the conduction band bottom energy X_1 at X-point , does not have obvious changes.
2. The conduction band bottom energy L_1 at L-point constantly decreases, when going from Si to Sn, the reduction rate is about 1. 5 eV.
3. It is noteworthy that the Γ-point conduction band bottom's energy $\Gamma_{2'}$ shows the trend of rapid decline with the increase of core state shell, the decline rate is about 4 eV.

The changing tendency of the three conduction band bottom energy not only indicates the Si, Ge and Sn conduction band bottom are located at (near) X, L and Γ point (α-Sn is already a zero band gap materials) and more, it indicates the importance of core states effects for the design of direct band gap materials. With the core states increases, the indirect band gap materials will be transformed to a direct band gap material. In the design of a direct band gap group IV alloys, selection of the heavier Sn atoms as the composition of materials will be inevitable. Recently, the electronic structures of SiC, GeC and SnC with a hypothetical zincblende-like structure have been calculated by Benzair and Aourag (Benzair & Aourag (2002)), the results also show that the conduction band bottom energy Γ_1 will reduced rapidly with the Si, Ge, Sn increasing core state, and eventually led to that SnC is a direct band gap semiconductor. From another perspective, the effect of the lattice constant on the band structure is with considerable sensitivity, which is a well-known result. Even if the identical material, as the lattice constant increases, the most sensitive effect is also contributed to rapid reduction of the conduction band bottom energy Γ (Corkill & Cohen (1993)). Therefore, for a composite material under normal temperature and pressure, a natural way to achieve larger lattice parameter is to choose the substituted atom with larger core states. From this point of view, the core states effect and the influence of lattice constant on the band structure have a similar physical mechanism. Figure 1(a) shows the core states effect, the size of the core states is indicated by a core-electron number $Z_c = Z - Z_v$, where Z is atomic number and Z_v the valence electron number.

3.2 Electronegativity difference effect

In the compound semiconductor, there are two kind of atoms which were bonded by so-called polar bond or partial polar bond, and this is directly related to their interatomic electronegativity difference. In pseudopotential theory, that is included in the antisymmetric part of the crystal effective potential. The variation trend of three conduction band bottom energies at Γ-, L- and X- point for two typical zinc blende semiconductors, Ga-V and III-Sb, with their interatomic electronegativity difference is shown in Figure 1 (b) and (c). Note that here the Pauling electronegativity scale (see Table 15 in Phillips. 1973) was selected, because it is particularly suitable for sp^3 compound semiconductors. It can be seen from the Figure 1(b-c), the Γ conduction band bottom energy will be rapidly reduced as the electronegativity difference decrease and then get to close to the Γ valence band top, so that GaAs, GaSb, and InSb in these two series compounds are of direct band gap semiconductors, whereas GaP and AlSb are the indirect band gap material due to a larger electronegativity difference. However, there is no theory available at present to quantitatively explain this change rule, moreover we note, using of other electronegativity scale (for example, Phillips's scale) , the variation rule is not so obvious. For all of these, the change tendency of semiconductor conduction band bottom energy under the Pauling electronegativity scale can still be taken as a reference to design the direct band gap material model.

The above two effects, core states and electronagativity difference effect, indicate that the direct and indirect bandgap properties in semiconductor within the same crystal symmetry have the characteristic change trend as follows:

- An atom with bigger core state is more advantageous to the composition of semiconducting material having a direct band gap.
- The compounds by atoms with a smaller electronegativity difference, are conducive to compound semiconductor transformation from indirect band gap to direct band gap.

These results may give us a sense that choosing the atomic species makes a design reference, but they cannot explain the existing data completely. For example the above two typical III-V series, have important exception:

1. For the series of AlN (d) AlP (ind) AlAs (ind) AlSb (ind) , only AlN is a direct gap semiconductor, but it has a largest electronegativity difference and a smallest core states, which are mutually contradictory with the first two effects. .
2. For the series of GaN (d) GaP (ind) GaAs (d) GaSb (d), the GaN is a direct band gap material, although the electronegativity difference is larger than that of GaP and the core states is smaller.

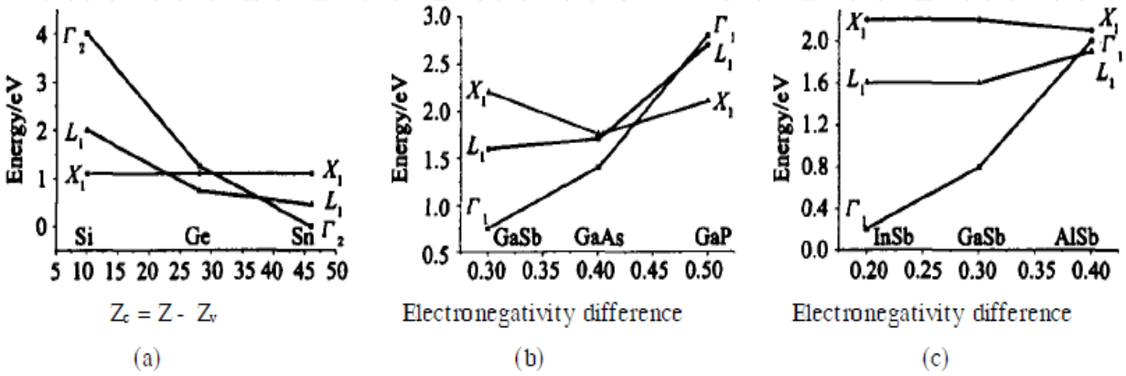

Fig. 1. The energies (Γ, X, L) at conduction band bottom vs (a) the electron number in core states for element semiconductors, and vs (b and c) the electronegativity difference between the component atoms in compound semiconductors.

This fact shows that the direct-indirect variation tendency of the band structure for these two series semiconducting material has another mechanism which needs be further ascertained.

3.3 Symmetry effect

In fact, the band gap type of AlN and GaN is different from their corresponding materials in that series, one of the important reasons is that they have different crystal symmetry. What kind of crystal symmetry can help the formation of a direct band gap of electronic structure in solids? This is the issue to be discussed in this section. In general, the electronic structure in solids depends on the electron wave function and crystal effective potential, in which the symmetry of the crystal unit cell is concealed. In order to reveal the connection between band gap type and crystal symmetry, we consider that now we can only use statistical methods to reveal the relationship, because there is no theoretical description for this issue at present. In Table 1, we list out both the point group symmetry and bandgap type for about 50 most common semiconductors. A careful observation will find out that some of variation tendency which so far has not been clearly revealed in this very ordinary table:

1. The unit cells of the main semiconductor materials have O_h, T_d, and C_{6v} point group symmetry, also they do not exclude other symmetry, such as D_{6h}, D_2 and so on. Let us make a simple statistical distribution for the crystal symmetry vs band-gap type. It can be seen that the materials have an O_h cubic symmetry and are all of indirect band gap, including II-VI group's CdS and CdS having a stable cubic structure O_h under high pressure (Benzair & Aourag 2002), although they have a C_{6v} symmetry and a direct

bandgap in normal pressure. In addition, I-VII group Ag halide, AgCl and AgBr have O_h symmetry though they are indirect band gap material. The only exception is α-Sn, but it is the zero direct band gap, which does not belong to semiconducting material in strict sense.

2. The materials which have hexagonal symmetry C_{6v} and D_2 symmetry, including the new super-hard materials BC_2N (Mattesini & Matar 2001), all have a direct band gap.

Group IV			III-V			II-VI			I-VII			Others		
SC	PG	d/i	SC	PG	d/i	SC	PG	d/i	SC	PG	d/i	SC	PG	d/i
C	O_h	i	BN	D_{6h}	i	ZnO	C_{6v}	d	CuCl	T_d	d	MnO	O_h	i
Si	O_h	i	BP	T_d	i	ZnS	C_{6v}	d	CuBr	T_d	d	NiO	O_h	i
Ge	O_h	i	BAs	T_d	i	ZnS	T_d	d	CuI	T_d	d	GaSe	D_{6h}	d
Sn	O_h	d/0	AlN	C_{6v}	d	ZnSe	T_d	d	AgCl	O_h	i	InSe	D_{6h}	d
SiC	T_d	i	AlP	T_d	i	ZnTe	T_d	d	AgBr	O_h	i	BC_2N	D_2	d
GeC	T_d	i	AlAs	T_d	i	CdS	C_{6v}	d	AgI	T_d	d			
SnC	T_d	d	AlSb	T_d	i	CdS	O_h	i	AgI	C_{6v}	d			
CSi_2Sn_2	D_2	d	GaN	C_{6v}	d	CdSe	C_{6v}	d						
CGe_3Sn	D_2	d	GaP	T_d	i	CdSe	O_h	i						
			GaAs	T_d	d	CdTe	T_d	d						
			GaSb	T_d	d	HgS	T_d	d						
			InN	T_d/ C_{6v}	d	HgSe	T_d	d						
			InP	T_d	d	HgTe	T_d	d						
			InAs	T_d	d									
			InSb	T_d	d									

Table 1. Point-group symmetry and band-gap type of crystals. Where SC=semiconductor, PG=point group and d/i=direct or indirect gap.

3. The materials which have zinc-blende structure symmetry, T_d and D_{6h} symmetry, are kind of between two band gap types, direct- and indirect gap, in which HgSe and HgTe reveal only a small direct band gap. If the relativistic corrections are included, they will be the semi-metal (Deboeuij et al. 2002). Now we temporarily ignore these facts. In the materials which have T_d and D_{6h} symmetry, there are an estimated ~75% belonging to direct bandgap semiconductors.

For convenience, we use the group order g of the point group of the crystal unit cell to describe the crystal symmetry, in which the point group T_d and D_{6h} have a same group order g (=24), and call it 'same symmetry class'. Let F_d be the percentage of direct band gap materials accounted for the material number of the same symmetry class. Statistical dependence of the F_d vs the group order g is an interesting diagram scheme, as shown in Figure 2. In this case, F_d=1 for the direct bandgap and F_d=0 for the indirect bandgap. This diagram indicats very explicitly that reducing the crystal symmetry or, the points group's operand is advantageous to the design and synthesis of the direct band gap semiconducting material. In fact, the Brillouin zone folding effect can also be seen as an important effect of lowering the symmetry of the crystal. For example, lower the symmetry from T_d to C_{6v}, the face-centered cubic Brillouin zone length Γ- L is equal to twice the Γ-A line of hexagonal Brillouin zone. In this case, the conduction band bottom L of T_d will be folded to the conduction band bottom Γ of C_{6v}, leading to a direct band gap. We note that the band gap

type will also be determined by the other factors, for example, the symmetry of electronic wave function at the conduction band bottom and the valence band top. Nevertheless, the main features of both the electronic structure and the band gap type are dominantly determined by crystal structure and their crystal potentials and charge density distribution that should be understandable.

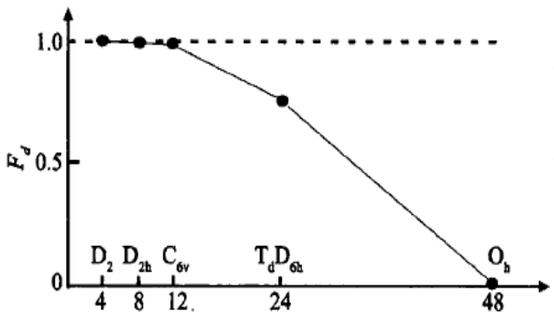

Fig. 2. A relationship between crystal symmetry and band gap type.

Note that the main statistical object in Fig.2 is sp^3 and sp^3-like hybridization semiconductor; it also includes some of ionic crystals and individual magnetic ion oxide compounds. It does not exclude increasing other more complex semiconducting material in the Table 1. However, we believe that the general changing trend of F_d has no qualitative differences. In other words, reducing the crystal symmetry is conducive to gain direct bandgap semiconductors. In addition, the semi-magnetic semiconductors, most of the magnetic materials and the transition metal oxides have a more complex mechanism. To determine their band gap type also needs to consider the spin degree of freedom, the strongly correlation effect, more complex effects and other factors. The topic needs to be investigated in the future.

4. Computational design: model

The design requirements are: the new material must be compatible with Si microelectronics technology; it contains Si to achieve lattice matching, and the material is of direct band gap so as to avoid the light-emitting process involving surface and/or interface state, so that the devices to provide the required functions for ultra-high-speed applications.

As stated above, in order to meet these requirements, the reduced symmetry principle can provide the direction of the crystal geometry design. We carry out energy band structure computation beforehand, so that the ascertainment on the crystal structure model has a reliable basis. There are two available essential methods to reduce the crystal symmetry:

Method 1: in the Si lattice, insert some non-silicon atoms to substitute part of silicon atoms, or produce silicon compounds (alloy), so as to reduce the crystal from O_h point group symmetry to T_d point group symmetry, or to D_{4h}, D_{2h} and other crystal structures with a lower symmetry.

Method 2: in the Si lattice, by using periodic insertion of non-silicon atom layer or Si alloy layer to obtain the lower symmetry materials.

The above two methods may realize the modification for the Si bandgap type. Among them, the method 2 is more suitable for the growth process requirements on Si(001) surface. for

example, in order to obtain a Si-based superlattice with symmetry lower than silicon crystal, the non-silicon atom monolayer can be grown on the silicon (001) surface, and then silicon atoms are grown, Repeatedly proceed this process by using Molecular Beam Epitaxy (MBE), Metal-Organic Chemical Vapour Deposition (MOCVD) or Ultra-high vacuum CVD (UHV-CVD), a new Si-based superlattice can be synthesized. In this way, we can not only reduce the symmetry of the silicon-like crystal, but also modify the bandgap type. This is a primarily method for the computational design.

On intercalated atoms choice, from the theoretical point of view, an inserted non-silicon atoms layer can lower the symmetry. The kinetics of crystal growth requires careful selection of insertion atoms, we consider here, the bonding nature of the Si atom with the inserting non-Si atoms. A natural selection on the insertion atoms is the IV-group atoms (C, Ge, Sn), the same group element with silicon, and the VI-group atoms (O, S, Se), due to the fact that they and Si atoms can form a stable thin film similar to SiO_2 film

We have performed a detailed study on electronic structure of two series of silicon based superlattice materials, which include $(IV_xSi_{1-x})_m/Si_n$ (001) superlattices (Zhang J L . et al. 2003; Chen et al.2007; Lv & Huang. 2010) and $VI(A)/Si_m/VI(B)/Si_m$ (001) superlattice series (Huang 2001a; Huang & Zhu . 2001b,c, Huang et al. 2002; Huang 2005).

4.1 $(Sn_xSi_{1-x})_m/Si_n$ (001) superlattices

The $(Sn_xSi_{1-x})_m/Si_n$ (001) superlattices we designed is composed of Sn_xSi_{1-x} alloy layer and Si layer, alternatively grown on Si (001) substrates. The unit cells of the $(Sn_xSi_{1-x})_m/Si_n$ (001) superlattices are shown in Figure 3 (a,b,c) for atomic layer mumber m=n=5 and x=0.125, 0.25, 0.5, respectively. Where Si_5 is a cubic unit cell which includes 5 Si atomic layers on Si(001) substrate. Similarly, the $(Sn_xSi_{1-x})_5$ is also a cubic Sn_xSi_{1-x} alloy on Si(001) surface. Although the Si and IVSi alloy are cubic crystals, the $(IV_xSi_{1-x})_5/Si_5$ (001) superlattices is a tetragonal crystal, the unit cell has a D_{2h} symmetry that is lower than cubic point group O_h. Note that the unit cell of this superlattice contains nine atomic layer along the [001] direction (c-axis) , because two cubes ($IVSi)_5$ and (Si_5) have common crystal faces. For simplicity, we present it in the following:

This structure will be named as $IV_xSi_{1-x}/Si(001)$. The equilibrium lattice constants after lattice relaxation of the superlattices and pure silicon have been obtained by means of total energy calculation within the DFT-LDA framework.

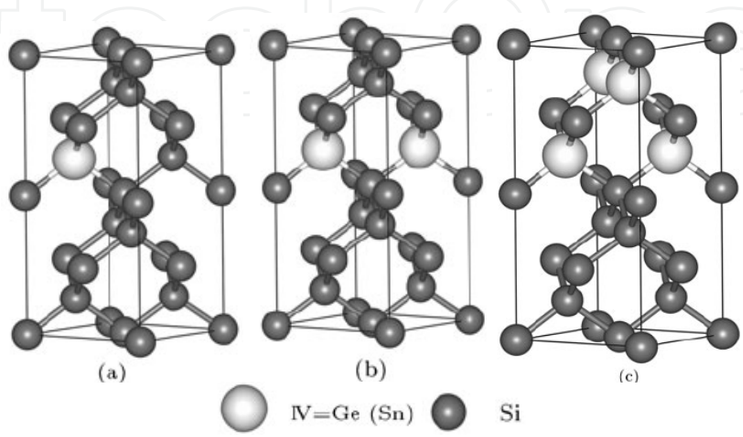

Fig. 3. The unit cell of $(IV_xSi_{1-x})_5/Si_5$ (001) superlattices. (a) x=0,125, (b) x=0.25, (c) x=0.5.

The results are shown in Table 2. From Table 2 we can find obviously that these superlattices have the reasonable lattice matching with the silicon. The lattice mismatch is less than 3% for a smaller IV component, e.g. for x< 0.25. The result indicates that epitaxy alloy (IVSi) on silicon (001) surface, (a IV-atom doped homogeneous epitaxy alloy), will be much easier to form than the heterogeneous epitaxy III-V compounds on silicon surface. The detailed calculation study shown that, although (IVSi) alloy is probably an indirect bandgap material, yet the IV_xSi_{1-x}/Si (001) superlattice composed of the Si and (IV_xSi_{1-x}) alloys might be a direct bandgap semiconductor with smallest bandgap located at Γ-point in Brillioun zone. Their electronic properties will be discussed in section 5.

Materials	*a*=*b*	*c*
Si	10.26	20.52
$Sn_{0.125}Si_{0.875}$/Si (001)	10.49	20.92
$Sn_{0.25}Si_{0.75}$/Si (001)	10,58	21.30
$Sn_{0.5}Si_{0.5}$/Si (001)	10.79	21.90
$Ge_{0.125}Si_{0.875}$/Si (001)	10.36	20.71
$Ge_{0.25}Si_{0.75}$/Si (001)	10,39	20.79
$Ge_{0.5}Si_{0.5}$/Si (001)	10.47	20.92

Table 2. The theoretical equilibrium lattice constants (in a.u.) of superlattices ($IV_xSi_{1-x})_5/Si_5$ (001) and a pure silicon.

4.2 VI(A)/Si_m/ VI(B)/Si_m (001) superlattices

Another new Si-based semiconductor we designed is VI(A)/Si_m/VI(B)/Si_m (001) superlattice, here VI(A) and VI(B) are VI-group element monolayer grown on silicon (001) surface, VI(A or B) =O , S or Se. In token of Si_m, index m is the silicon atomic layer number. The superlattice structure can be grown epitaxially on silicon (001) surface, layer by layer, and then a VI-group atomic monolayer is epitaxially grown as an inserted layer. In the epitaxial growth process, the location of VI-group atoms is dependent on the silicon (001) reconstructed surface (i.e., dimerization) mode, while the surface atoms of the dimerization are also dependent on the number of silicon layers. For example, in the case of m=6 or even number, it has a simple (2x1) dimerization (Dimer) structure, whereas in m=5 or odd number, a (2x2) dimerization (Dimer) structure will be obtained. Therefore, we have two unit cells with different symmetry; they are orthogonal and tetragonal superlattice, respectively. The unit cell models for m=5 and m=10 are shown in Figure 4. It can be shown that the two structures models have been avoided dangling bonds in bulk. From the perspective of chemical bonds, each silicon atom has four nearest neighbor bonds, whereas each VI atom has two nearest neighbour Si-VI bonds. They form a stable structure, and prevent the participation of interface states. The designed models of superlattice unit cells, VI(A)/Si_5/VI(B)/Si_5 and VI(A)/Si_{10}/VI(B)/Si_{10} are shown in Figure 4, in which the inserted VI atoms layer is a periodic monolayer and the dimer reconstruction on surface has been considered. Note that the primitive lattice vectors of the superlattices are different from the ($Sn_xSi_{1-x})_5/Si_5$ (001) due to the Si(001) surfaces having been restructured. During the first-principles calculations, the distance between the VI-atoms and Si-atoms, the positioning of the VI-atoms parallel to the interface with respect to the Si (001) surface and the lattice parameters of the superlattice cell can be varied. After the relaxations are finished, the total energy of the relaxed interface system is at the lowest, then a stable unit cell will be

obtained. The theoretical equilibrium lattice constants (in a.u.) of the superlattices are given in Table 3. It can be seen that the $a \approx b$ for tetragonal structure superlattice VI(A)/Si_5/VI(B)/Si_5(001) with (2x2) dimer, whereas the VI(A)/Si_6/VI(B)/Si_6(001) is an orthogonal structure superlattice with (2x1) dimer. In all cases, these superlattices formed by alternating a VI-atom monolayer and diamond structure Si along to [001] direction, their lattice parameters are increased with the core states of inserted VI-atoms increased.

Materials	*a*	*b*	*c*
Se/Si_5/O/Si_5(001)	14,62	14.53	33.07
Se/Si_5/S/Si_5 (001)	14.64	14.59	34.28
Se/Si_5/Se/Si_5 (001)	14.66	14.66	34.79
Se/Si_6/O/Si_6(001)	14,42	7.31	38.57
Se/Si_6/S/Si_6 (001)	14.47	7.33	39.80
Se/Si_6/Se/Si_6 (001)	14.53	7.33	40.27

Table 3. The theoretical equilibrium lattice constants (in a.u.) of the superlattices VI(A)/Si_m/VI(B)/Si_m (001).

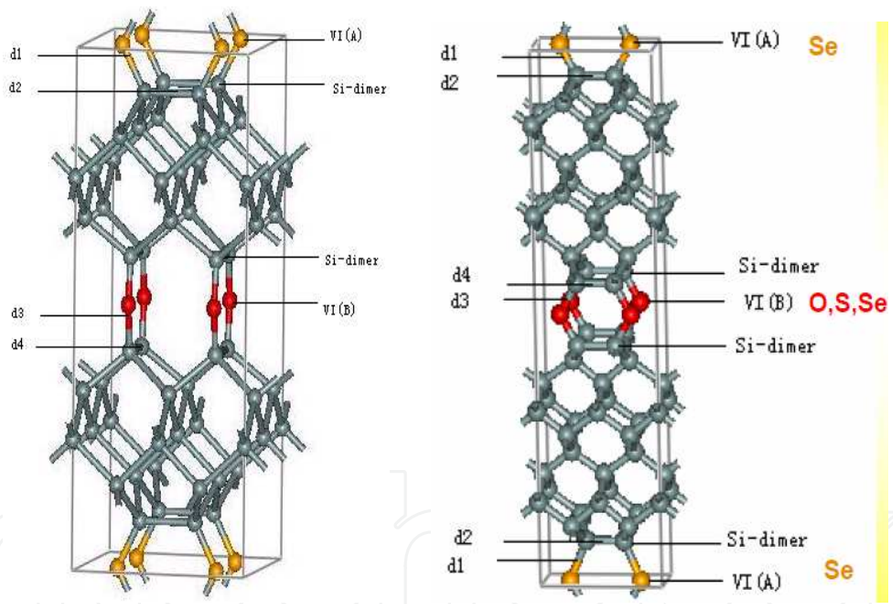

Fig. 4. The model of designed superlattice unit cell. The inserted VI atoms layer is a monolayer, the dimer reconstruction on surface has been considered. (a) VI(A)/Si_5/VI(B)/ Si_5(001). (b) VI(A)/Si_{10}/VI(B)/Si_{10}(001).

5. Results and discussion

According to our computational design principle, the theoretical superlattices IV_xSi_{1-x} / Si (001), (IV=Ge,Si; x=0.125,0.25,0.5) and VI(A)/Si_m/ VI(B)/Si_m (001) (VI=O,S.Se; m=5.6.10) have been investigated. In our calculations, the band structures based on the density functional theory (DFT) and local density approximation (LDA) are performed first. The

purpose is to find and demonstrate the direct bandgap materials. On this basis, in order to correct the Kohn-Sham band gap which is always underestimate due to the LDA limitation, a representative quasiparticle band structure calculation in Hedin's GW approximation was carried out. The calculation in details and main results are described below.

5.1 Electronic structure of IV_xSi_{1-x} / Si (001) superlattices

The DFT-LDA calculation for these new superlattices is based on a total energy pseudopotential plane-wave method. The wavefunctions are expressed by plane waves with the cutoff energy of $|k+G|^2 \leq 450$ eV. The Brillouin zone integrations are performed by using 6x6x3 k-mesh points within the Monkhorst-Pack scheme. The convergence with respect to both the energy cutoff and the number of k-point has been tested. With a larger energy cutoff or more k points, the change of the total energy of the system is less than 1 meV. Calculated equilibrium lattice constants after lattice relaxation are given in Table 2, and it is very closely Vegard's law for different IV component.

The Band structures of Ge_xSi_{1-x}/ Si (001) and Sn_xSi_{1-x}/ Si (001) superlattices are shown in Fig.5(a,b) for x=0.125, 0.25 and 0.5., respectively. It can be seen that the Ge_xSi_{1-x}/ Si (001) (x=0.125 and 0.25) and Sn_xSi_{1-x}/ Si (001) (x=0.125) are the superlattices with a direct gap at Γ-point. Although the dispersion relation of the valence band is quite similar in all cases, the lowest conduction band revealed great differences in the dispersion. The reason is that both the Ge and Sn have a larger core states and hence larger lattice parameters than that of Si, Their perturbation potential will change the Kohn-Sham effective potential V_{eff} and eigenvalues $E^{KS}(k)$. As Corkill-Cohen has pointed out (Corkill & Cohen M.L (1993)), the result is that the lowest conduction band (Γ-band edge of Si) will continue to lower with the increase of lattice constant. This feature can lead to an above three Γ- point direct band gap superlattice, of course, also there is a greater possibility in transforming them to direct band gap material due to the lower symmetry of the unit cells. In the same way, with the Sn superlattice band gap becoming small compared with the Ge is understandable.

We note that the selection of superlattice primitive cell is not unique. If the location of alternative atoms Ge, Sn are chosen symmetrically for the unit cell center, a D_{4h} symmetry superlattice can be obtained. In order to examine the energy band structure in this case, the band structures of Sn_xSi_{1-x}/ Si (001) superlattices are calculated again. In the same time, as a comparison, the band structure of pure Si (in D_{4h}) is also given in Figure 6(a). The results show that silicon is still an indirect band gap semiconductor, the conduction band bottom is in Γ-X and Γ-Z line, and only Sn_xSi_{1-x}/ Si (001) (x = 0.125) is a direct band gap material. The results excellently agree with Figure 5 (b). The shift of conduction band edge for these systems is also clearly visible when we inspect going from Si to $Sn_{0.5}Si_{0.5}$/Si(001) superlattice. First of all, the energy of Γ-band edge is reduced and hence the direct gap superlattice $Sn_{0.125}Si_{0.875}$/Si(001) is formed. Then, the reduction of Z-band edge exceeds that of the Γ-band edge (if Sn component increased), the indirect gap superlattices are obtained, with smaller relevant band gap.

The Kohn-Sham band gap E_g^{KS} of the superlattices are summarized in Table 4, the data is corresponding to different model and exchange-correlation approximation quasi-particle energy E^{QP} and quasi-particle wavefunction ψ^{QP}, the key-point is calculated. In order to correct the Kohn-Sham band gap E_g^{KS} of the superlattices, the quasiparticle band structure within Hedin's GW method (GWA) is performed by using PARATEC and ABINIT packages, for a representative superlattice $Sn_{0.125}Si_{0.875}$/Si(001), where G is a one-particle Green function, W is a dynamic screening Coulomb interaction. The quasi-particle energy

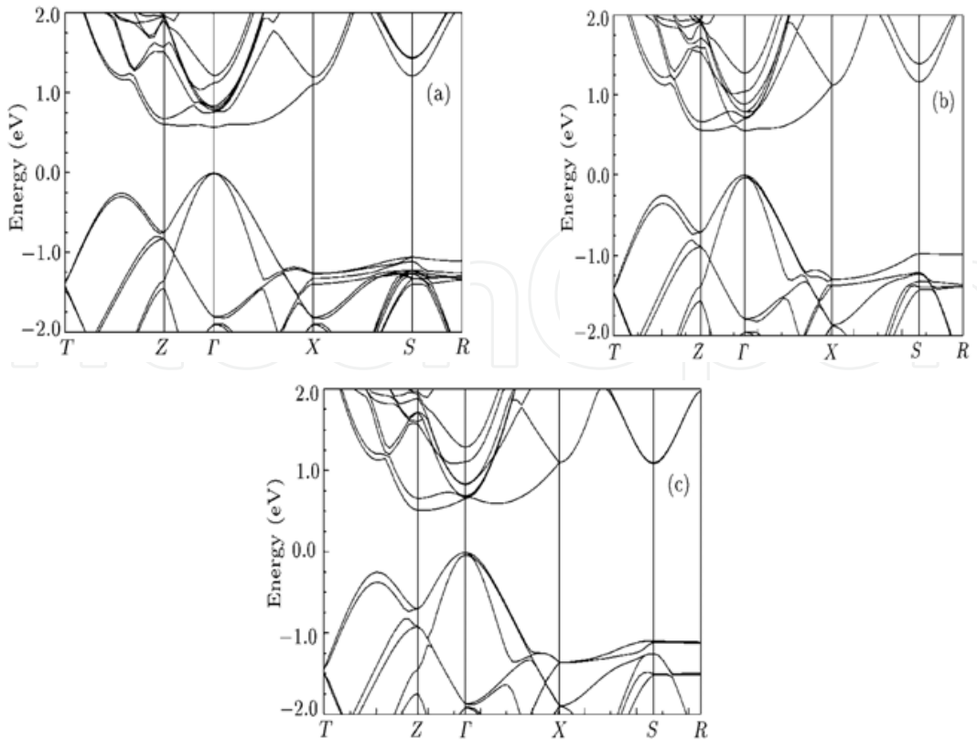

Fig. 5(a). Band structure of Ge_xSi_{1-x}/ Si (001) superlattices. (a)x=0.125, (b) x=0.25, (c)x=0.5

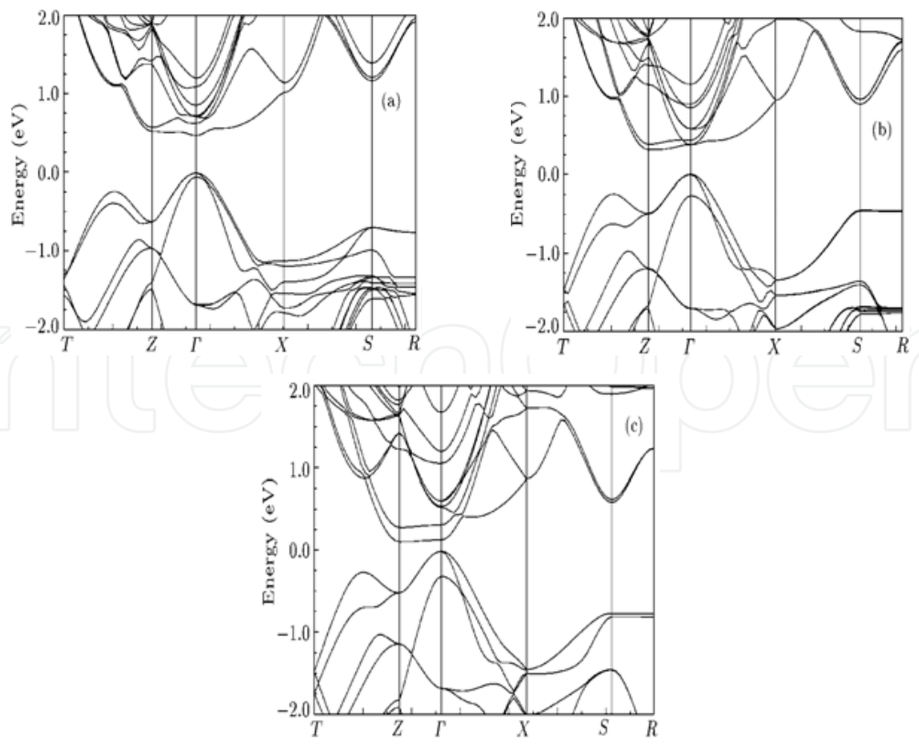

Fig. 5(b). Band structure of Sn_xSi_{1-x}/ Si (001) superlattices. (a)x=0.125, (b) x=0.25, (c)x=0.5

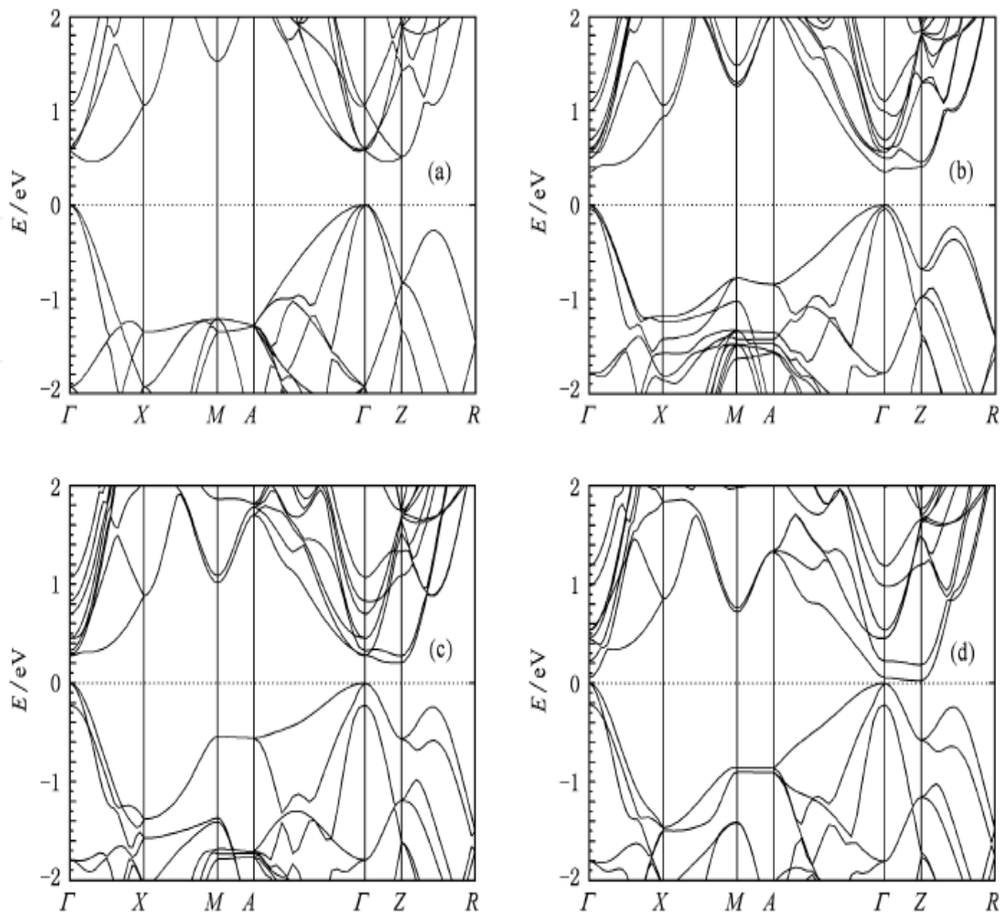

Fig. 6. DFT-LDA band structures of Si and Sn_xSi_{1-x}/ Si (001) superlattice in D_{4h} symmetry.(a) Si, (b,c,d) superlattices for x=0.125, 0.24, 0.5, respectively.

E^{QP} and quasi-particle wavefunction ψ^{QP} are solutions of quasi-particle equation which contains an electron self-energy operator $\sum$. One of key-points is to calculate the $\sum$. In Hedin's GWA, $\sum$ = iGW, it does not consider vertex corrected. The extensive research points out (Hybertsen M.S.& Louie S.G. 1985, 1986), the quasi-particle wave function ψ^{QP} is almost completely overlapped with the Kohn-Sham wave function ψ^{KS}, the overlap range exceeds 99.9%. Therefore, in our GWA calculation, we will assume that can use Kohn-Sham wave function as quasi-particle wave function of zero-level approximation. Therefore, we can construct the Green function G that employ the Kohn-Sham wave function ψ^{KS}, based on the Kohn-Sham equation solutions. The dynamic screening Coulomb interaction W depends on the bare Coulomb interaction v and dielectric function matrix χ. The dielectric matrix calculation is also a difficult task, we adopt the simpler RPA approximation. In this way, based on the KS equation solutions, we could solve the quasi-particles equation and obtain the quasi- particle band structure of the superlattice. As a representative result of IV_xSi_{1-x}/Si(001) superlattices, a quasi-particle band structure is given in Figure 7, which is quite similar to its LDA band structure in Figure 6(b). The main difference is that the direct band gap increases from E_g^{LDA} = 0.35 eV to E_g^{QP} = 0.96 eV. In other words, the quasi-particle bandgap correction of this system is 0.61 eV. Although G and W has not carried out self-

consistent calculation in present work, one can see that the result is quite accurate and reliable,

Materials	$E_g^{KS}(D_{2h}$, GGA)	$E_g^{KS}(D_{4h}$,LDA)	$E_g^{QP}(D_{4h}$, G_0W_0)
Si	0.58	0.46	
$Sn_{0.125}Si_{0.875}$/Si(001)	0.47 (Γ-Γ)	0.35 (Γ-Γ)	0.96 (Γ-Γ)
$Sn_{0.25}Si_{0.75}$/Si(001)	0.31 (Γ- Z)	0.21 (Γ- Z)	
$Sn_{0.5}Si_{0.5}$/Si(001)	0.10 (Γ- Z)	0.03 (Γ- Z)	
$Ge_{0.125}Si_{0.875}$/Si(001)	0.57 (Γ-Γ)		
$Ge_{0.25}Si_{0.75}$/Si(001)	0.55 (Γ-Γ)		
$Ge_{0.5}Si_{0.5}$/Si(001)	0.51 (Γ- Z)		

Table 4. Band gap E_g (in eV) of the IV_xSi_{1-x}/Si(001) superlattices. (Γ-Γ) stands for direct gap at Γ, GGA the generalized gradient approximation, LDA the local density approximation.

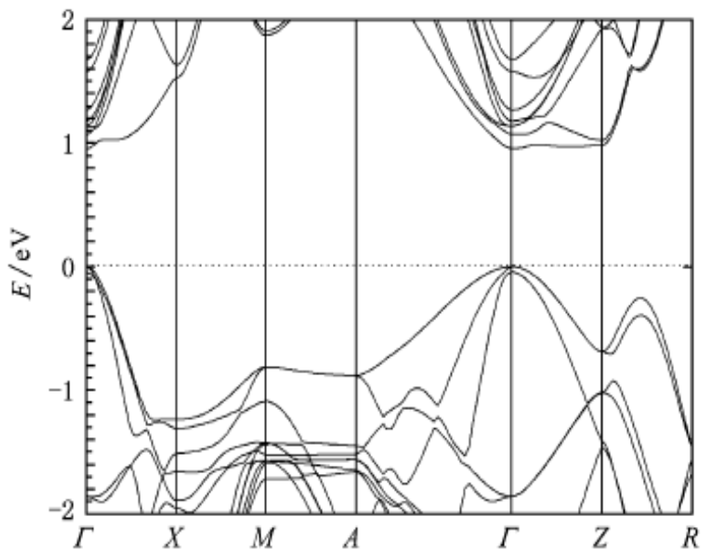

Fig. 7. Quasiparticle energy band of $Sn_{0.125}Si_{0.875}$/Si(001) superlattice.

In fact, this approach is often called G_0W_0 method in the literature. But by this method, results obtained are better for the *sp* semiconductors even than partial self-consistent method G_0W and GW_0 as well as the complete self-consistent method GW. There are already some works studying the reasons for these facts (e.g. see Ishii et al. 2010).

5.2 Electronic structure of VI(A)/Si $_m$/ VI(B)/Si $_m$ (001) superlattices

Another series of computational designed silicon-based superlattice is VI(A)/Si $_m$/ VI(B)/Si $_m$ (001), which includes O/Si_m/O/Si_m(001), S/Si $_m$/S/Si $_m$ (001), Se/Si $_m$/Se/Si $_m$ (001), Se/Si $_m$/O/Si $_m$ (001), and Se/Si $_m$/ S/Si $_m$ (001) etc for m=5,6,and 10. The results show that, for the cases of selected VI (A) = Se, VI (B) = O, S, Se, the direct band gap superlattices can be formed. Two unit cell structure models, tetragonal and orthogonal structure for m=5 (or odd number) and m=10 (or even number) are shown in Figure 4. These stable lattice structure models and their equilibrium lattice constants, the VI-Si bond length and

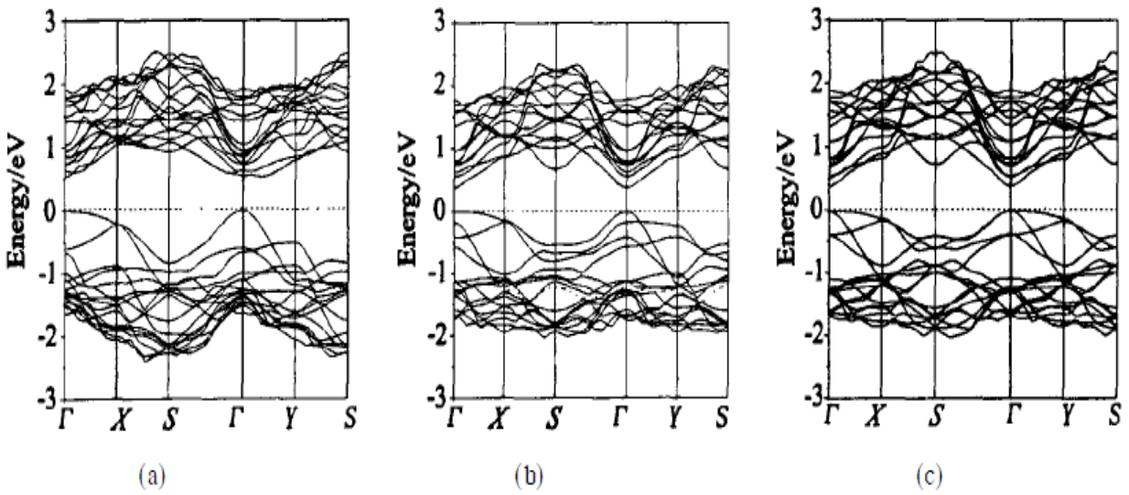

Fig. 8. Band structures of Si-based superlattices with odd number layers Si and tetragonal structure. (a) $Se/Si_5/O/Si_5(001)$, (b) $Se/Si_5/S/Si_5(001)$ (c) $Se/Si_5/Se/Si_5(001)$.

bond angle are calculated by using the first principles total energy method. The DFT-LDA band structure calculation of the Si-based superlattices use mixed-basis pseudopotential method with norm- conservation pseudopotential (Hamann et al 1979) and VASP package with ultra-soft pseudopotential (Kresse & Furthmüller 1996) and Ceperly- Alder Exchange-correlation potential (Ceperley & Alder 1980), respectively. The wavefunctions are expanded by plane waves with the cutoff energy of 12 Ry which has been optimized via total energy tolerance ΔE=1 meV.

The band structures of $Se/Si_5/VI(B)/Si_5(001)$ (VI(B)=O,S,Se) superlattices with a tetragonal structure are shown in Figure 8. It is shown that the materials are the potential Si-based optoelectronic semiconductors with Γ-point direct gap.

The band structures of $O/Si_5/VI(B)/Si_5(001)$ (VI(B)=O,S) which only involve the VI-atoms of smaller core-states, are also studied and found that are the quasi direct gap materials with the X-point valence band top (Huang 2001a; Huang & Zhu 2001b,c, Huang et al. 2002; Huang 2005)., although their smallest direct band gap is still at Γ- point.

To investigate the influence of $Se/Si_m/VI(B)/Si_m(001)$ (VI(B)=O,S,Se) with even number layers silicon that have the orthogonal structures on the electronic properties and band gap type, the $Se/Si_m/VI(B)/Si_m(001)$ (VI(B)=O,S,Se; m=6,10) are calculated with the same method. The results indicate that they are also direct band gap superlattices as shown in Figure 9. In other words, band-gap type and number of layers of silicon in $Se/Si_m/VI(B)/Si_m(001)$ (VI(B)=O,S,Se) are not sensitively dependent. However, choosing the appropriate size of the VI atoms, such as Se, is important. Using Se and O or S periodic cross intercalation in Si(001), the desired results can be achieved more satisfactorily (Zhang J.L. Huang M.C. et al, (2003)) due to the core states effect and the smaller electronegativity difference. The LDA band gap of these Si-based materials is listed in Table 5. For the tetragonal structure material (m=5), its band gap is a little bit bigger than that of the orthogonal structure situation (m=6,10). As well known, the LDA band gap is not a real material band gap, since the exchange correlation potential in DFT-LDA equation can not correctly describe the excited states properties. In order to revise LDA band gap, we can use GWA methods or screen-exchange-LDA (sX-LDA) method to solve the quasiparticle equation. The existed research shows that this energy gap revision is quite large, for example, for

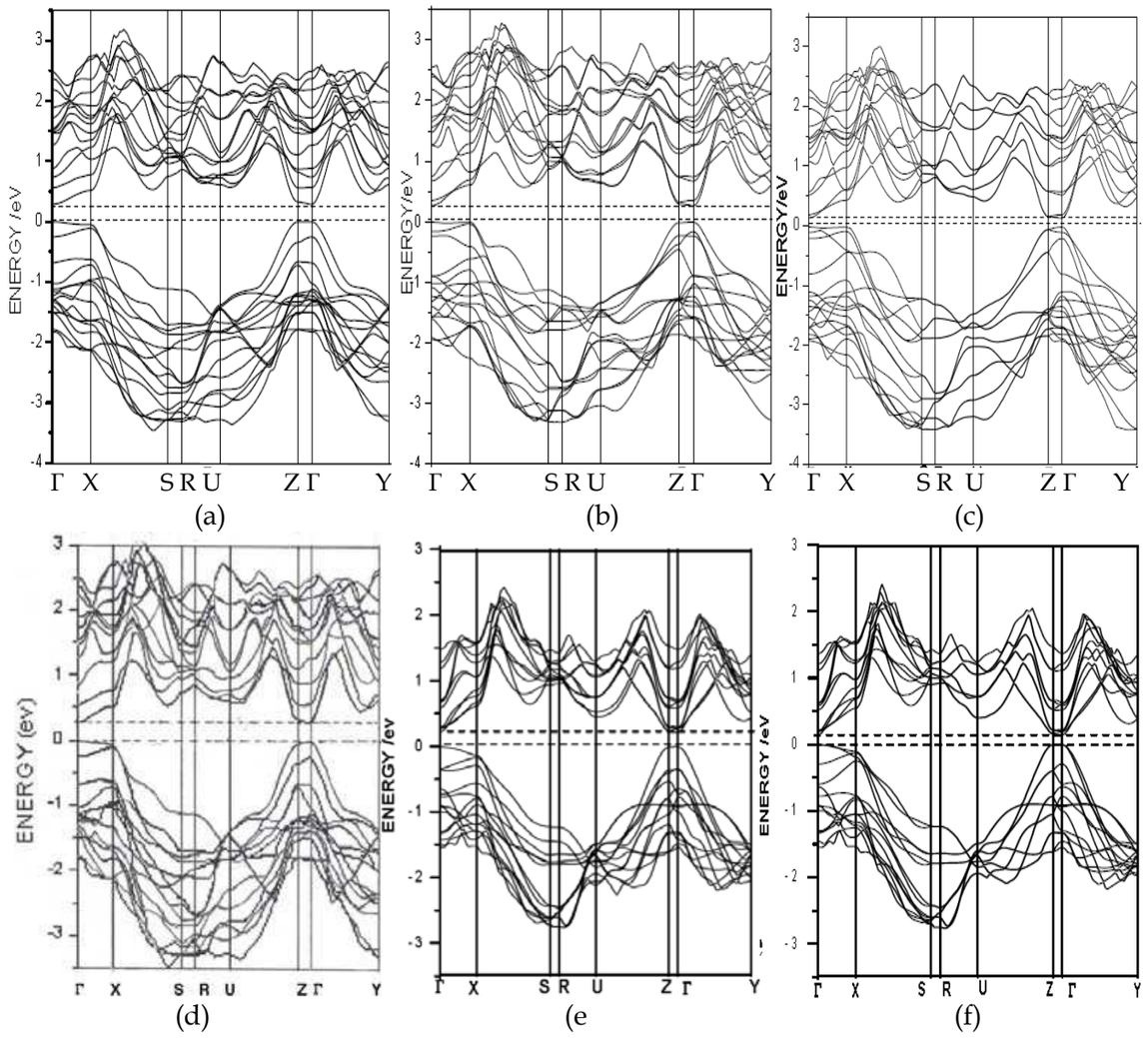

Fig. 9. Band structures of Si-based superlattices with even number layers Si in orthogonal structure. (a) $Se/Si_6/O/Si_6(001)$, (b) $Se/Si_6/S/Si_6(001)$, (c) $Se/Si_6/Se/Si_6(001)$, (d) $Se/Si_{10}/O/Si_{10}(001)$, (e) $Se/Si_{10}/S/Si_{10}(001)$, (f) $Se/Si_{10}/Se/Si_{10}(001)$.

Materials	E_g^{KS}(LDA, Tet)	E_g^{KS}(LDA,Orth.)
$Se/Si_5/O/Si_5(001)$	0.50	
$Se/Si_5/S/Si_5(001)$	0.40	
$Se/Si_5/Se/Si_5(001)$	0.35	
$Se/Si_6/O/Si_6(001)$		0.30
$Se/Si_6/S/Si_6(001)$		0.25
$Se/Si_6/Se/Si_6(001)$		0,20
$Se/Si_{10}/O/Si_{10}(001)$		0.30
$Se/Si_{10}/S/Si_{10}(001)$		0.25
$Se/Si_{10}/Se/Si_{10}(001)$		0,20

Table 5. Band gap E_g (in eV) of the $Se/Si_m/VI(B)/Si_m(001)$ (VI(B)=O,S,Se) superlattices.

silicon and germanium, It is about 0.7 and 0.75 eV, respectively (Hybertsen M.S. and Louie S.G. (1986)). Our GWA calculation for IVSi/Si superlattice has the band gap revision of 0.61 eV, which is near to Silicon. Taking into account the quasi-particle band gap correction, for example, 0.61 eV, the band gap of these si-based materials is in the region of 1,11-0.81 eV, which is corresponding to the infrared wavelength of 1.12-1.53μm, just matching to the windows of lower absorption in the optical fiber. Therefore they are potentially good Si-based optoelectronic materials.

Similar to our computation cited above, MIT's research group (Wang et al 2000) had provided a class of semiconductors, in which a particular suitable configuration, $(ZnSi)_{1/2}P_{1/4}As_{3/4}$, is identified that lattice constant matched to Si and has a direct band gap of 0.8 eV. Although this material has good performance, but its complex structure, involving the four elements in the heteroepitaxy on silicon substrates, the crystal growth may have much more difficulties.

Another well-known computational design is proposed by Peihong Zhang etc (Zhang P.H, et al. 2001). They suggest two IV-group semiconductor alloys CSi_2Sn_2 and CGe_3Sn that have body-centered tetragonal (bct) structure, the lattice matched with Silicon. Among them, CSi_2Sn_2 has a direct band gap located at X point in the BZ, and CGe_3Sn has a Γ- point direct band gap, because its lattice is slightly distorted from b.c.t,, the crystal symmetry of CGe_3Sn is lower than that of CSi_2Sn_2. Their GW band gap is in 0.71-0.9eV range. Anyway, they are also potential contenders of Si-based optoelectronic materials. The heterogeneous epitaxy of these IV group alloys on silicon substrate is not an easy task, because the positions of the component atoms have to meet some particular requirements in these alloys. In contrast, we use of periodic atomic intercalation method to have more practical application prospect. The symmetry reduction principle, core states effect and electronegativity difference effect can be used not only for silicon-based materials but also can be extended to other indirect band gap semiconductor systems, such as AlAs, diamond and other materials, to realize the energy band modification. They also have a significant research and development prospect. We designed Si-based optoelectronic materials can natural be realized lattice matched with silicon substrate. The growth process on the MBE, MOCVD or UHV-CVD might easier to control. Once the experimental research of these materials is brokenthrough, OEIC technology will have a significant development.

6. Conclusion

This chapter has given an overview of our works on the computational design of a new class of Si-based optoelectronic materials. A simple effective design idea is presented and discussed. According to the design ideas, two series models of superlattice are constructed and calculated by the first principles method. It is found that the superlattices Ge_xSi_{1-x}/Si(001) (x=0.125,0.25), Sn_xSi_{1-x}/Si(001) (x=0.125), $Se/Si_m/VI/Si_m/Se(001)$ (VI=O,S,Se; m=5,6.10) are the Γ-point direct energy gap Semiconductors, moreover, they can be realized lattice matched with silicon substrate on (001) surface. These new materials have the band gap region of 0.63-1.18 eV under the GW correction that is corresponding to infrared wavelength of 1.96-1.05 μm and are suited for the applications in the optoelectronic field. An open question for all kind of Si-based new materials is what and how to do to achieve them under the experimental research.

7. Acknowledgments

This work was supported by the Chinese National Natural Science Foundation in the Project Code: 69896260, 60077029, 10274064, 60336010. Author wishes to thank Dr. T.Y. Lv, Dr. J. Chen and Dr. D.Y.Chen for their calculation efforts successively in these Projects. We also are grateful to Prof. Q.M.Wang and Prof. Z.Z. Zhu for many fruitful discussions. Finally, author want to express his thanks to Prof. Boxi Wu for reading the Chapter manuscript and gave valuable comments.

8. References

Aryasetiawan F , Gunnarsson O. (1998), The GW method .*Rep. Prog. Phys*. ,61 :p.237.

Aulbur W G, Jonsson L ,Wilkins J W. (2000), Quasiparticle calculations in solids. *Solid State Physics* ,54 :p.1-231.

Benzair A ,Aourag H. (2002), Electronic structure of the hypothetical cubic zincblende-Like semiconductors SiC, GeC and SnC . *Phys. Stat . Sol*. (b) , 231 (2) : p.411-422.

Buda F. et al, (1992), *Phys. Rev. Lett*.,69,p.1272

Canham L T. (1990), Silicon quantum wire array fabrication by electrochemical dissolution of wafer . *Appl. Phys. Lett* . 57 :p.1 045 - 1 048.

Ceperley D M ,Alder B I. (1980), Ground state of the elect ron Gas by a stochastic method. *Phys. Rev. Lett* .45 :p.566.

Chen J. Lv T,Y. Huang M.C.(2007), Electronic structure of $Si_{1-x}IV_x$/Si superlattices on Si(001), *Chin.Phys. Lett*. 74,p.811.

Corkill J.L and Cohen M.L (1993), Band gaps in some group-IV materials: A theoretical analysis, *Phys. Rev*.B47,p.10304

Cullis A G, Canham L T. (1991), Visible light emission due to quantum size effects in highly porous crystalline silicon . *Nature* , 353 :p.335 - 338.

Deboeuij Y P L , Kootstra F J, Snijders G. (2002), Relativistic effects in the optical response of HgSe by time-dependent density functionals theory. *Int, J. Quantum Chem.* , 85 :p.450 - 454.

Ennen H, Schneider J, Pomerenke G,Axmann A. (1983) 1.54μm luminescence of erbium-implanted III-V semiconductors and silicon, *Appl. Phys. Lett*. 43, p.943.

Hamann D R , Schluter M , Chiang C. (1979), Norm-conserving pseudopotentials . *Phys. Rev. Lett* .,43, p.1 494.

Hirschman K D, Tsybeskov L, Duttagupta S P, et al. (1996), Silicon-based light emitting devices integrated into microelectronic circuits . *Nature* , 384 :p.338 - 340.

Hohenberg P.and Kohn W. (1964). Inhomogeneous electron Gas .*Phys. Rev*. 136 p.B864,:.

Huang M.C. (2001a), The new progress in semiconductor quantum structures and Si-based optoelectronic materials, . *J. Xiamen Univ.(Natural Sci.)* , 40 , p. 242 -250.

Huang M.C. and Zhu Z. Z. (2001b), An exploration for Si-based superlattices structure with direct-gap . *The 4th Asian Workshop on First principles Electronic Structure Calculations*.. p.12.

Huang M.C. and Zhu Z. Z.(2001c), A new Si-based superlattices structure with direct band-gap. *Proc. of 5th Chinese Symposium on Optoelectronics*. p.44 - 47.

Huang M.C, Zhang J L ,Li H P ,et al. (2002), A computational design of Si-based direct band-gap materials. *International J . of Modern Physics* B 16 :p.4 279 - 4 284.

Huang M.C,(2005), An ab initio Computational Design of Si-based Optoelectronic Materials, *J. Xiamen Univ.(Natural Sci.)* , 44 , p. 874

Hybertsen M.S. and Louie S.G. (1985). First-Principles Theory of Quasiparticles: Calculation of Band Gaps in Semiconductors and Insulators, *Phys. Rev. Lett*. 55, p.1418

Hybertsen M S ,Louie S G. (1986), Electron correlation in semiconductors and insulators . *Phys. Rev*. B34 :p.5 390 - 5 413.

Hybertsen M.S. and Schluter M. (1987), Theory of optical transitions in Si/Ge(001) strained-layer superlattices, *Phys. Rev*. B36, p.9683

Ishii S., Maebashi H. and Takada Y. (2010), Improvement on the GWT Scheme for the Electron Self-Energy and Relevance of the G_0W_0 Approximation from this Perspective. *arXiv* [*cond-mat,mtrl-sci*] 1003.3342v2

Kohn W AND Sham L J. (1965), Self-consistent equations including exchange and correlation effects. Phys. Rev. 140 : p.1 133.

Kresse G.and Furthmüller J. (1996), Efficient iterative schemes for *ab initio* total-nenrgy calculations using a plane-wave basis set. *Phys.Rev*. B54, p.11169

Lu Z H ,Lockwood D J ,Baribeau J M. (1995), Quantum confinement and light emission in SiO_2/Si superlattice . *Natur,* 378 :p.258 - 260.

Lv T.Y. Chen J. Huang M.C. (2010), Band structure of Si-based superlattices $Si_{1-x}Sn_x$/Si. *Acta Phys. Sinica*, 59,p.4847

Mattesini M ,Matar S F. (2001), Search for ultra-hard materials :theoretical characterisation of novel orthorhombic BC_2N crystals . *Int . J . Inorganic Materials* , 3 : p.943 -957.

Mooser E ,Pearson W B. (1960),The chemical bond in semiconductors. *Progress in Semiconductors* ,5 : p.141 -188.

Nassiopoulos A G, Grigoropoulos S , Papadimit riou S. (1996),Electroluminescent device based on silicon nanopillars . *Appl. Phys. Lett* .69 :p.2 267 - 2 269.

Ng W.L ,Lourenc M A ,Gwilliam R M et al. (2001), An efficient room-temperature silicon-based light emitting diode .*Nature* , ,410 :p.192 - 194.

Pavesi L ,Dal Negro L ,Mazzoleni C ,et al. (2000), Optical gain in silicon nanocrystals. *Nature* , ,409 :440 - 444.

Petersilka M , Gossmann U I , Gross E K U. (1996), Excitation energies from time-dependent desity functional theory . *Phys. Rev. Lett* .76 :p.1 212.

Phillips J C. (1973) *Bonds and Bands in Semiconductors*. USA : Academic Press ,.

Rosen Ch H ,Schafer B ,Moritz H ,et al. (1993) Gas source molecular beam epitaxy of $FeSi_2$ / Si (111) heterostructures . *Appl. Phys. Lett* .,62 :p.271.

Runge E , Gross E K U. (1984), Density functional theory for time-dependent systems . *Phys. Rev. Lett* .,52 :p.997.

Seidl A, Gorling A, Vogl P, et al. (1996), Generalized Kohn-Sham schemes and the band-gap problem . *Phys. Rev*.,B53 :p.3 764.

Walson W L, Szajowski P F, Brus L E. (1993), Quantum confinement in size-selected surface-oxidised silicon nanocrystals . *Science* , 262 :p.1 242 - 1 244.

Wang T, Moll N, Kyeongjae Cho, Joannopoulos J. D. (2000) Computational design of compounds for monolithic integration in optoelectronics, *Phys. Rev*. B63, p.035306

Zhang J.L.,Huang M.C. et al, (2003), Design of direct gap Si-based superlattice VIA/Si_m/VIB / Si_m/ViA. *J. Xiamen Univ.(Natural Sc.,)*,42 :p.265 - 269.

Zhang P.H, Crespi V H, Chang E, et al. (2001), Computational design of direct-bandgap semiconductors that lattices-match silicon. *Nature* , 409 :p.69 - 71.

Zhang Q , Filios A ,Lofgren C ,et al. (2000), Ultrastable visible electroluminescence from crystalline c-Si/O superlattice. *Physica* , E8 :p.365 - 368.

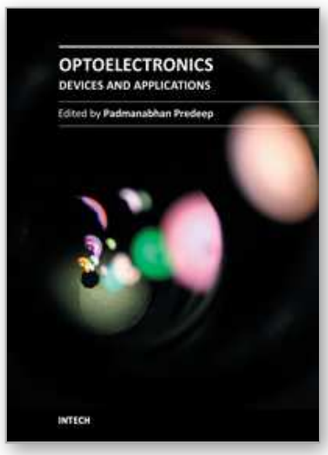

Optoelectronics - Devices and Applications

Edited by Prof. P. Predeep

ISBN 978-953-307-576-1
Hard cover, 630 pages
Publisher InTech
Published online 03, October, 2011
Published in print edition October, 2011

Optoelectronics - Devices and Applications is the second part of an edited anthology on the multifaced areas of optoelectronics by a selected group of authors including promising novices to experts in the field. Photonics and optoelectronics are making an impact multiple times as the semiconductor revolution made on the quality of our life. In telecommunication, entertainment devices, computational techniques, clean energy harvesting, medical instrumentation, materials and device characterization and scores of other areas of R&D the science of optics and electronics get coupled by fine technology advances to make incredibly large strides. The technology of light has advanced to a stage where disciplines sans boundaries are finding it indispensable. New design concepts are fast emerging and being tested and applications developed in an unimaginable pace and speed. The wide spectrum of topics related to optoelectronics and photonics presented here is sure to make this collection of essays extremely useful to students and other stake holders in the field such as researchers and device designers.

INTECH
open science | open minds

InTech Europe
University Campus STeP Ri
Slavka Krautzeka 83/A
51000 Rijeka, Croatia
Phone: +385 (51) 770 447
Fax: +385 (51) 686 166
www.intechopen.com

InTech China
Unit 405, Office Block, Hotel Equatorial Shanghai
No.65, Yan An Road (West), Shanghai, 200040, China
中国上海市延安西路65号上海国际贵都大饭店办公楼405单元
Phone: +86-21-62489820
Fax: +86-21-62489821

IntechOpen